Study on the photodegradation behaviors of thermal-aged silk

Yuxuan Gong[1,2], Guangzhao Zhou[2], Chengquan Qiao[2*] and Yongkang Pan[2]

Abstract

In museums, silk cultural relics are highly sensitive to light. However, lighting is inevitable due to the exhibition needs, despite any light would pose irreversible damage to silk. Although the solution of eliminating UV radiation was widely achieved in museum lighting environment, long-time accumulation of other light sources still would induce photo-degradation of silk. This work therefore established the simulated light ageing experiments to assess the degradation behaviors of silk samples with different ageing degrees. The variation of color values and structure transformation of each sample group were determined by the means of scanning electron microscopy (SEM), colorimeter, Fourier Transform infrared spectroscopy (FTIR) and ^{13}C CPMAS NMR. The results indicated that silk samples with different initial ageing degrees presented different discoloration tendency and structural variation in experimental lighting environment, suggesting the higher disordered structure makes the silk more vulnerable to light damage. It is of great significance to understand the long-time impacts of illumination on degraded silk and further provide methodology for predicting the duration of exhibited silk cultural relics.

Keywords Silk, Light ageing, Degradation behavior, Photodegradation

Introduction

Silk is a carrier of culture, art and technology which represents one of the significant achievements of human civilization [1]. Silk fiber is a natural polymer composed of fibroin which forms the core of the thread, and the glue-like sericin that connecting and surrounding two fibroins [2]. Prior to weaving, the majority of sericin is normally removed through degumming process [3, 4], which leaves mainly silk fibroin. And fibroin consists of amino acids that fold into crystalline region and amorphous region [5]. The amorphous region makes up of two subunits, which are a light chain and a heavy chain [6]. The highly ordered heavy chain consists of 12 hydrophobic domains containing repeated $(GAGAGS)_n$ amino acid sequences that ensures the heavy chain's resistance to humidity, heat, light, and other degradation factors [7–9]. The light chain connected to the heavy chain by disulfide bonds, is an independent sub-unit that with less stable properties and higher degradation rate [9]. Hence silk is a natural fiber that highly sensitive to environmental impacts.

Silk has been used for centuries in producing numerous historic textiles [10, 11]. Due to undergo various degradations in burial, such as oxidation, hydrolysis, pyrolysis etc., the unearthed silks are normally brittle. Subsequently, the physical environmental factors in museums, including humidity, temperature, air quality and lighting may cause secondary damage to silk cultural relics [12, 13]. Amongst them, the first three indexes can be adjusted by temperature control system, dehumidifier, and air purifier, to make it in favor of the preservation and conservation of silk [14, 15]. However, museum lighting environment is one of the most complex building light environments with multi-requirements, including visual pleasure and photoaging prevention [16]. The spectrum

*Correspondence:
Chengquan Qiao
qiaochengquan@ustc.edu.cn
[1] Institute of History of Science and Technology, Jiangsu University of Science and Technology, 666 Changhui Road, Zhenjiang 212100, China
[2] Basic Scientific Research Center for Cultural Heritage Conservation, University of Science and Technology of China, 96 Jinzhai Road, Hefei 230026, China

Gong *et al. Heritage Science*   (2024) 12:151

Page 2 of 13

of museum light sources consists of primarily the visible light with a wavelength of 380–780 nm, including a small quantity of UV radiation (wavelength < 400 nm) and IR radiation (wavelength ˃ 760 nm) [13]. Due to the exhibition needs, lighting is inevitable in museums despite any light would pose threats to silk [17].

In consideration of the correlations between materials of cultural relics and light exposure, artifacts such as silk and paper are categorized as high-light-sensitive exhibits that vulnerable to irreversible damage from optical radiation of lighting [13, 16]. Discoloration of textile and paper in relation to the dyes and pigments were extensively studied [18–21], including those particularly focused on the impacts of different light sources on color fading of paper and silk artifacts [17, 22]. Tan and Dang reviewed researches on light influence of highly sensitive artworks and indicated color change is one aspect of degradation, while the mechanism of lighting deterioration in regard to the changes of chemical composition and molecular structure is necessary to be studied by employing accelerated photoaging experiments [13]. And in line with the points, UV-induced degradation of silk was studied to evaluate the secondary structure transformation [23, 24], changes of structure and isotope ratios [25], and color and structure variation [12]. It can be seen from previous research that the discoloration of light-sensitive artifacts under various light sources has been widely studied since color change is commonly an obvious sign of light ageing. Compared with other visible light sources, silk is more vulnerable to UV radiation due to the higher energy of UV [13]. Hence, previous studies of UV-induced degradation have focused not only on the fading of silk, but also on the structural variation of silk. As a result, the solution of reducing UV radiation was normally achieved by installing UV-blocking filters on light sources and windows, or equipping with LED lamps in modern museums [13]. However, photochemical reactions are complex, filtering out ultraviolet light is not entirely safe to ancient silks, particularly long-time accumulation of other light sources would still trigger photoaging of silk. Therefore, it is essential to investigate the impacts of long exposure of museum lighting on silk cultural relics by establishing the degradation mode on color variation and structure transformation of silks, thus to fill the knowledge gap.

As proposed by International Commission of Illumination (CIE), the aim of the conservation policy of museum lighting is to maintain a certain annual exposure limit, measured in lux·hour (lx·h) [26, 27]. According to the recommendations of 'Code for Lighting Design of Museum' of China (GB/T 23863–2009) [28], the high-light-sensitive exhibits such as silk, should be maintained at standard illuminance value ≤ 50 lx, and the annual exposure limit (AEL) is set at 50,000 lx·h, based on which

museums estimate the number of annual exposures for certain exhibits. This study therefore established the simulated photoaging experiments based on the estimated annual exposure of museum lighting, and the deterioration behaviors of silk from macroscopical to microcosmic were determined by the means of SEM, colorimeter, FTIR and ^{13}C CPMAS NMR. It overall aims to better understand the long-time impacts of luminous environment on degraded silk and further provide methodology for predicting the duration of silk cultural relics.

Materials and methods
Preparation of aged silk samples
Thermal ageing
Thermal ageing is commonly employed in accelerated ageing studies by applying elevated temperature to increase the degradation rate [4, 29, 30]. Refer to our previous study [31], the dry thermo-oxidation ageing temperature was set at 200 ℃ to between the glass transition temperature (178 ℃) and the initial decomposition temperature (220 ℃) of silk. Considering the silk collections in museums are with various degrees of ageing, the accelerated thermal ageing experiments were performed for different duration of time.

The commercial raw silks were cut into 10 cm × 3 cm size, thermal ageing experiments were lasted for 5 h, 10 h, 20 h, 30 h respectively.

Although the archeological conditions of silk relics cannot be accurately replicated, the artificial ageing experiments could simulate the natural degradation to some extent.

Light ageing
The series of silk samples with different pre-ageing degrees were placed into the SN-500F Xenon lamp ageing test chamber, the spectral distribution of the light sources is presented in Fig. 1. The ultraviolet filter was equipped to eliminate UV radiation (wavelength < 400 nm) and the light-accelerated ageing experiments were performed at a constant temperature of 20 ℃, 50% RH (which proved to be the most appropriate preservation conditions for silk cultural relics), and illuminance value of 100,000 lx (in accordance with AEL, artificial ageing for 1 h simulates the museum light exposure of 2 years). The samples were aged for 12 h a day, respectively 0 h, 6 h, 12 h, 24 h, 48 h, 72 h, 96 h, 120 h and 144 h in total.

Scanning electron microscopy (SEM)
Silk samples light-aged for 0 h, 48 h, 96 h, 144 h were selected and mounted onto a double-sided adhesive carbon tape set on aluminum stubs and were sprayed with gold for electric conduction. SEM analysis was performed on a ZEISS GeminiSEM 500 scanning electron
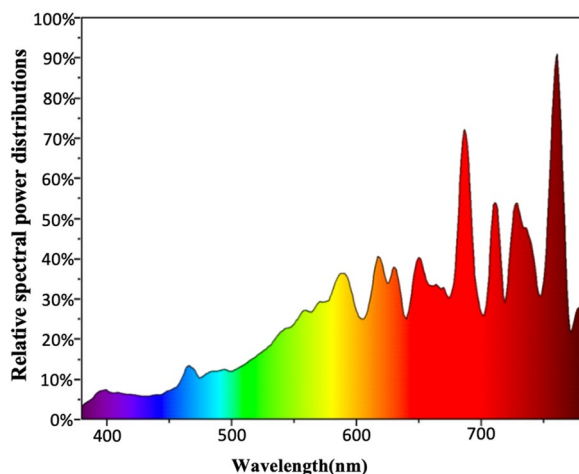
Gong *et al. Heritage Science*   (2024) 12:151

Page 3 of 13

Fig. 1 The spectral distribution of the light sources of Xenon lamp

microscope to characterize the microstructure of samples before and after light ageing.

Colorimeter

Colorimetric measurements were carried out by a NH300+computerized color spectrometer, and parameters were provided in CIE $L^*a^*b^*$ color space. The values of L^*, a^*, b^* were determined individually according to CIE 1976 scale [20]: L^* indicates lightness, which 0–100 represents the brightness from black to white; a^* indicates red and green, which negative and positive values indicate green and red respectively; b^* indicates yellow and blue, which negative and positive values indicate blue and yellow respectively. Five measurements were taken at different points for each sample and mean values were automatically obtained. The color difference (ΔE) was calculated by using the following equation (Eq. 1).

$$\Delta E = \sqrt{\left(\Delta L^*\right)^2 + \left(\Delta a^*\right)^2 + \left(\Delta b^*\right)^2} = \sqrt{\left(L^* - L^*_0\right)^2 + \left(a^* - a^*_0\right)^2 + \left(b^* - b^*_0\right)^2} \tag{1}$$

FTIR

FTIR measurements were conducted on a Thermo Scientific Nicolet 8700 FTIR spectrometer. Spectra were acquired in transmission mode and collected over a 4000 to 400 cm^{-1} range with 4 cm^{-1} resolution and 128 scans.

^{13}C CPMAS NMR

^{13}C CPMAS NMR analyses were performed by a Bruker AVANCE NEO 600 spectrometer operating at 600.16 MHz on proton and 150.92 MHz on carbon, equipped with a 3.2 mm CPMAS probe. Silk samples were packed and spun at the magic angle spinning rate of 22 kHz. Spectra were taken using cross-polarization pulse sequence, the 90° pulse was 2.6 μs with a relaxation

delay of 2 s. 2048 scans were accumulated and externally referenced to tetramethylsilane.
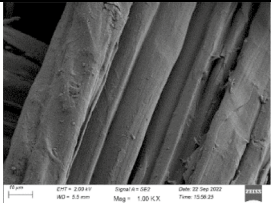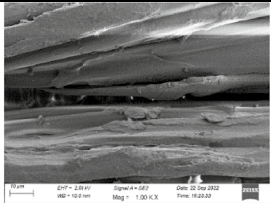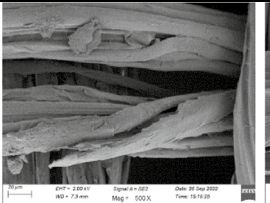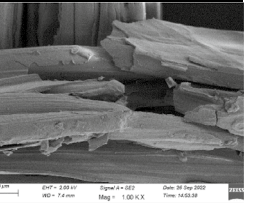
Results and discussion
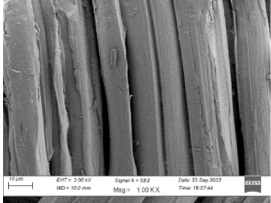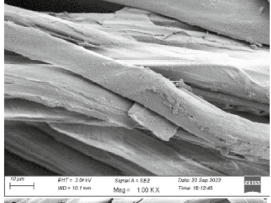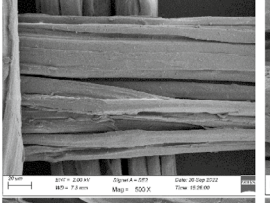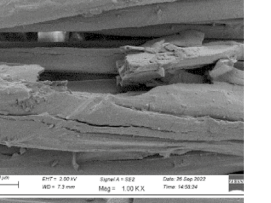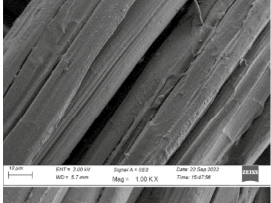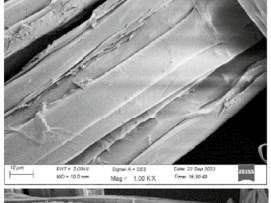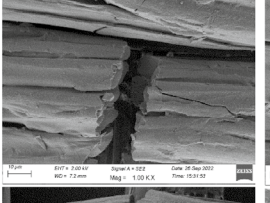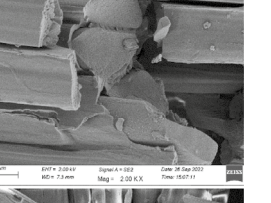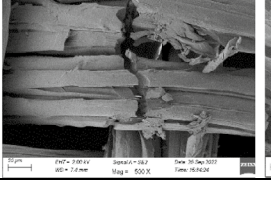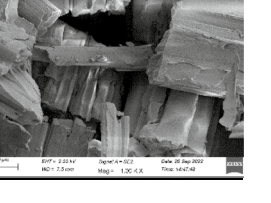
Morphological comparison

SEM is a useful tool in determining the morphological characteristics of degraded silk. As presented in Table 1, silk samples prior to light ageing had generally arranged fibers and tight structure. After light radiation, the degradation characteristics of roughness, cracks, fractures, fibrillations and other phenomena appeared in the microscopic morphology of silk samples, indicating deterioration was induced by the accelerated lighting reaction. And silk with higher initial ageing degree shows more severe damage at an earlier stage of illumination. It can be seen that significant fiber fractures are presented in the morphology of 30 h pre-aged silks by underwent 48 h of light ageing, while the surface of silk became rough and loose in other sample series but the integrity of the silk fibers was still maintained. After 96 h of exposure to lighting conditions, samples with different pre-ageing degrees exhibit more distinct levels of degradation. In particular, those silks with 20 h and 30 h of pre-ageing exhibited extensive fiber breakage. And the silks were delicate after completing 144 h of light ageing. It was found in the morphology of 5 h and 10 h pre-aged samples that fractures were obvious perpendicular to the fiber axis and cracks generated along the fiber axis. Meanwhile, it was also presented that 20 h and 30 h pre-aged silks were severely broken, cavities were formed inside the monofilament and gave rise to the partially peel of the fibers, suggesting that silks with higher initial ageing degree are more susceptible to photochemical reaction.

Colorimetry analysis

Color difference is an effective indicator in quantitatively assessing photodegradation. As shown in Fig. 2, the color variations of silk samples with different initial ageing degrees are distinct under same lighting environment. At the early stage of exposure, the brightness variations of silk samples were generally prominent (Fig. 2a). The brigh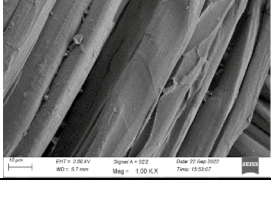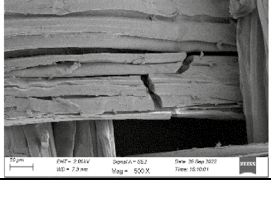tness of lower initial-aged silks increased approximate linearly with increasing exposure time. Whereas the brightness of higher initial-aged samples raised first, then went down suggesting that the whitening of severely aged silk is less obvious. As presented in Fig. 2b, the lower initial-aged silks tended to less red color, conversely, the higher initial-aged samples tended to strong red color.

Gong *et al. Heritage Science* (2024) 12:151

Page 4 of 13

Table 1 SEM images of the artificial aged samples with different ageing degrees

The variation of a^* was significant at the early stage, and gradually stable at a later time. It could be seen from Fig. 2c that the higher initial-aged samples exhibited prominent yellowing effect in the early stages of exposure, and the shift of b^* values levelled off latterly. While the lower initial-aged silk presented a negative shift in b^* values indicating less yellow color. As observed in Fig. 2d, the chromatic aberration curves of the samples have some overlaps. The color difference of the samples raised with the increase of the exposure time in the beginning, and fluctuated after approximately 20 h exposure. It can be seen that ΔE values exceeded 6 would cause visually noticeable color change, while ΔE values exceeded 12 resulting in significantly noticeable differences in color [13, 20].

According to the color values and chromatic aberration, silk samples with different initial ageing degrees revealed different color variation rate and discoloration tendency. Especially at the early stage of illumination, the difference in the colorimetric parameter variations was more significant due to the rapid photochemical reaction. To further study the deterioration process and mechanism of silk in molecular terms, FTIR and ^{13}C CPMAS NMR analyses were conducted.

FTIR analysis

FTIR analysis was utilized to determine the chemical and structural changes in each sample group. Figure 3 depicted FTIR spectra of the silk samples with varying degrees of photoaging within the range of 400 to 4000 cm^{-1}. The primary regions associated with the amid I (1600–1700 cm^{-1}), the amid II (1500–1600 cm^{-1}) and the amid III (1190–1300 cm^{-1}) are important for assess the structural transformation of silk [12, 25]. The characteristic absorption bands of the silk samples are provided in Table 2. The absorption bands at region 1648–1655 cm^{-1}, 1516–1529 cm^{-1}, and 1229–1233 cm^{-1} are assigned to the amid I (C=O stretching vibration, α-helix/random coil), amid II (C-N stretching and C-N-H bending vibrations), and amid III (C-N stretching and
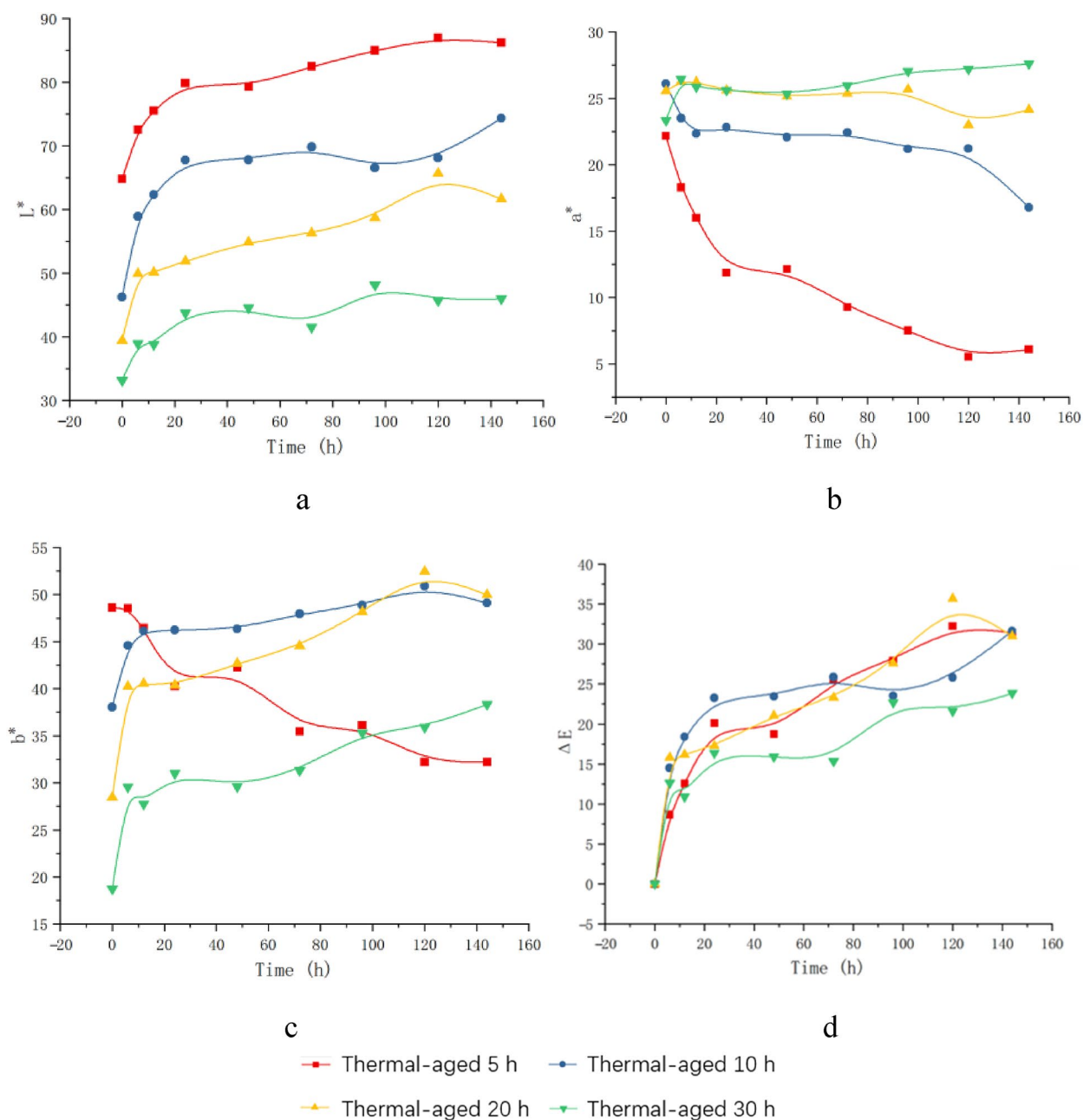
Fig. 2 Variation of the color values (**a**. L*, **b**. a*, **c**. b*, **d**. ΔE) of the samples with different ageing degrees

N–H bending vibrations, random coil/α-helix), respectively. It can be seen through the comparison of the amid I, amid II and amid III bands representing different exposure times that there are variations in the peak height and position presumably indicating the loss of peptide structure and the transformation from higher-ordered to disordered conformation of the samples as the ageing process advanced [12, 23, 32]. In order to further assess the structural transformation of the samples under experimental lighting, multiple indexes were employed to investigate the ageing behaviors. According to the previous studies [33], the absorption peaks at 1260 and 1230 cm^{-1} (amid III) are associated with β-sheet and random coil conformation respectively, for which the ratio of these integrated peaks (A_{1260}/A_{1230}) could be applied to define crystallinity degree of silk.

The examples of the spectra deconvolution and fitting of amide III band for each sample group are presented in
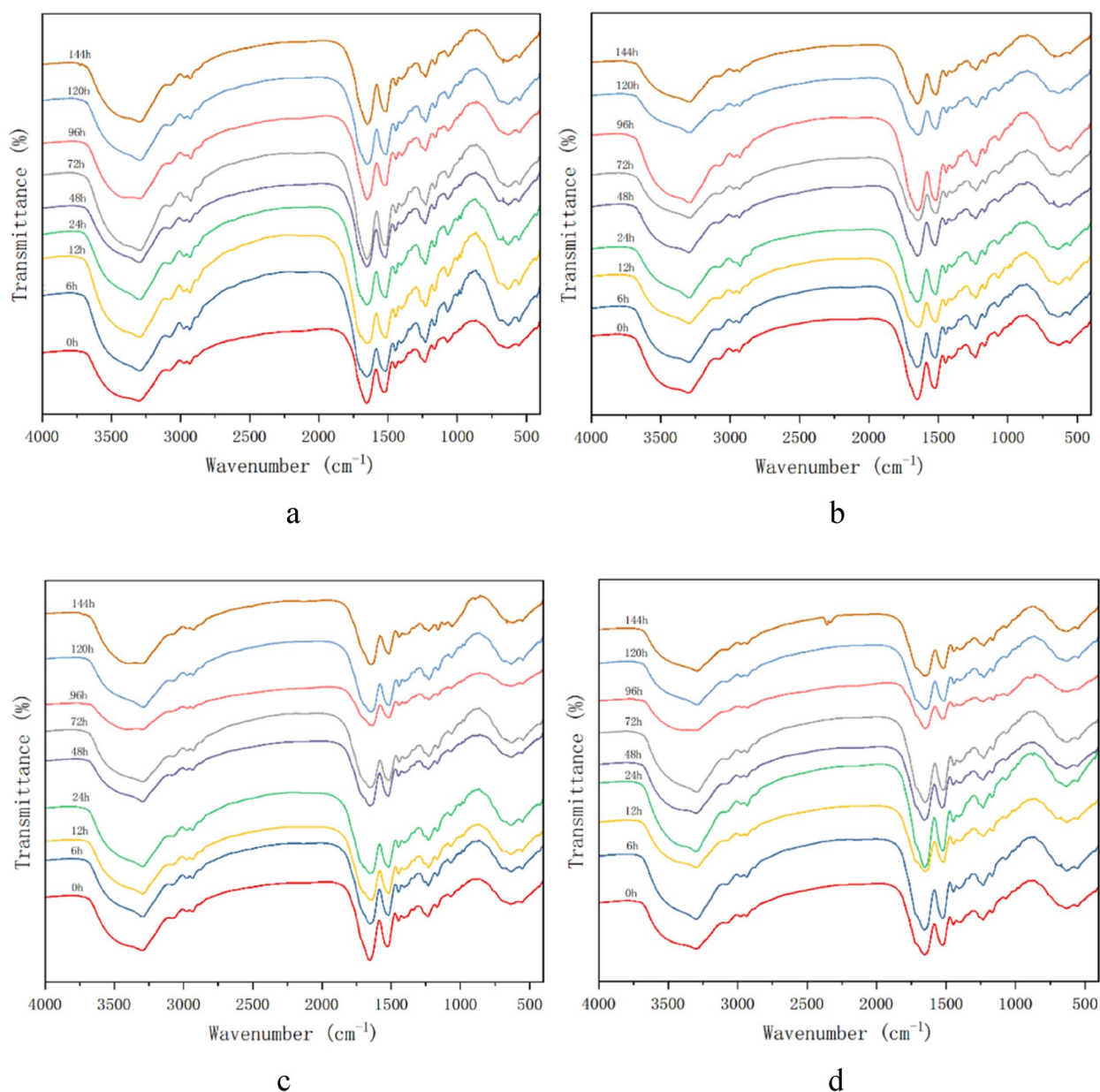
Fig. 3 FTIR spectra of each sample group (**a**. thermal-aged 5 h, **b**. thermal-aged 10 h, **c**. thermal-aged 20 h, **d**. thermal-aged 30 h) under different illumination time

Table 3. And the variation of the secondary conformation and crystallinity for the artificially aged samples are given in Fig. 4. As presented in Table 3, and Fig. 4a and b, the contents of random coil conformation slightly increased while the contents of β-sheet conformation showed a minor decrease with extending the exposure time. It is speculated that the experimental lighting conditions can induce the change of the secondary structure of silk, where light would break the bonding between the hydrogen bonds and result in the cleavage and reorganization of polypeptide chains [25]. Since β-sheet conformation and random coil conformation are mainly distributed in the crystalline region and the amorphous region respectively, the crystalline region is gradually destroyed upon photoaging leading to the conversion of β-sheet conformation to random coil conformation, and an increase in the content of random coil conformation in the amorphous region.

The distinct variation rate of secondary structure is observed in the silk samples with different pre-ageing

Table 2 Locations of the characteristic absorption bands in FTIR spectra

Exposure time (h)	Thermal-aged 5 h			Thermal-aged 10 h			Thermal-aged 20 h			Thermal-aged 30 h		
	amid I (cm⁻¹)	amid II (cm⁻¹)	amid III (cm⁻¹)	amid I (cm⁻¹)	amid II (cm⁻¹)	amid III (cm⁻¹)	amid I (cm⁻¹)	amid II (cm⁻¹)	amid III (cm⁻¹)	amid I (cm⁻¹)	amid II (cm⁻¹)	amid III (cm⁻¹)
0	1655	1522	1233	1652	1519	1233	1655	1529	1233	1654	1522	1232
6	1655	1516	1230	1652	1519	1232	1651	1519	1232	1654	1519	1232
12	1648	1516	1229	1652	1516	1230	1651	1517	1230	1652	1519	1231
24	1655	1516	1230	1652	1518	1231	1651	1518	1229	1652	1522	1232
48	1652	1518	1231	1654	1519	1231	1651	1519	1231	1655	1528	1232
72	1655	1519	1232	1652	1519	1231	1654	1519	1231	1654	1519	1231
96	1655	1529	1233	1655	1519	1232	1651	1519	1230	1652	1523	1233
120	1655	1519	1231	1654	1519	1231	1651	1518	1230	1652	1519	1230
144	1652	1519	1232	1652	1519	1231	1651	1518	1232	1652	1520	1232

Gong *et al. Heritage Science*   (2024) 12:151

Page 8 of 13

Table 3 Examples of the spectra deconvolution and fitting of the amide III band of each sample group

duration of thermal-ageing \ duration of light-ageing	0 h	48 h	96 h
5 h	β-sheet 31.79% / Random coil 68.21%	β-sheet 31.43% / Random coil 68.57%	β-sheet 30.97% / Random coil 69.03%
10 h	β-sheet 31.53% / Random coil 68.47%	β-sheet 30.31% / Random coil 69.69%	β-sheet 29.95% / Random coil 70.05%
20 h	β-sheet 31.19% / Random coil 68.81%	β-sheet 30.09% / Random coil 69.91%	β-sheet 29.56% / Random coil 70.44%
30 h	β-sheet 31% / Random coil 69%	β-sheet 29.83% / Random coil 70.17%	β-sheet 29.31% / Random coil 70.69%

degree. The distribution of secondary conformation varied slowly in lower initial-aged samples. While the conversion rate of β-sheet conformation to random coil conformation raised with the increase of the sample's initial ageing degree. During ageing process, degradation occurred priorly in the amorphous region, then both the amorphous and crystalline regions were destroyed as ageing advanced [12]. It is inferred that the amorphous region of higher initial-aged samples was severely destroyed with the crystalline region exposed and susceptible to the experimental lighting, resulting in a higher rate of photoaging.

The similar results are observed in the variation of crystallinity of the silk samples which exhibiting a decrease with slight fluctuation upon accelerated light ageing. During the pre-ageing process of thermal treatment, the damage occurred firstly in the amorphous region of silk, leading to the high index of crystallinity. After being subjected to light exposure, both the amorphous and crystalline regions were destroyed concurrently at an early stage, resulting in an obvious reduction of crystallinity. The variation of crystallinity was positively associated with the initial ageing degree of silk, that is, the higher the initial ageing degree, the more rapid the decrease of crystallinity. It is speculated that the higher initial-aged sample is with the disordered structure and severely destroyed amorphous region, while the amorphous region is no longer consolidates
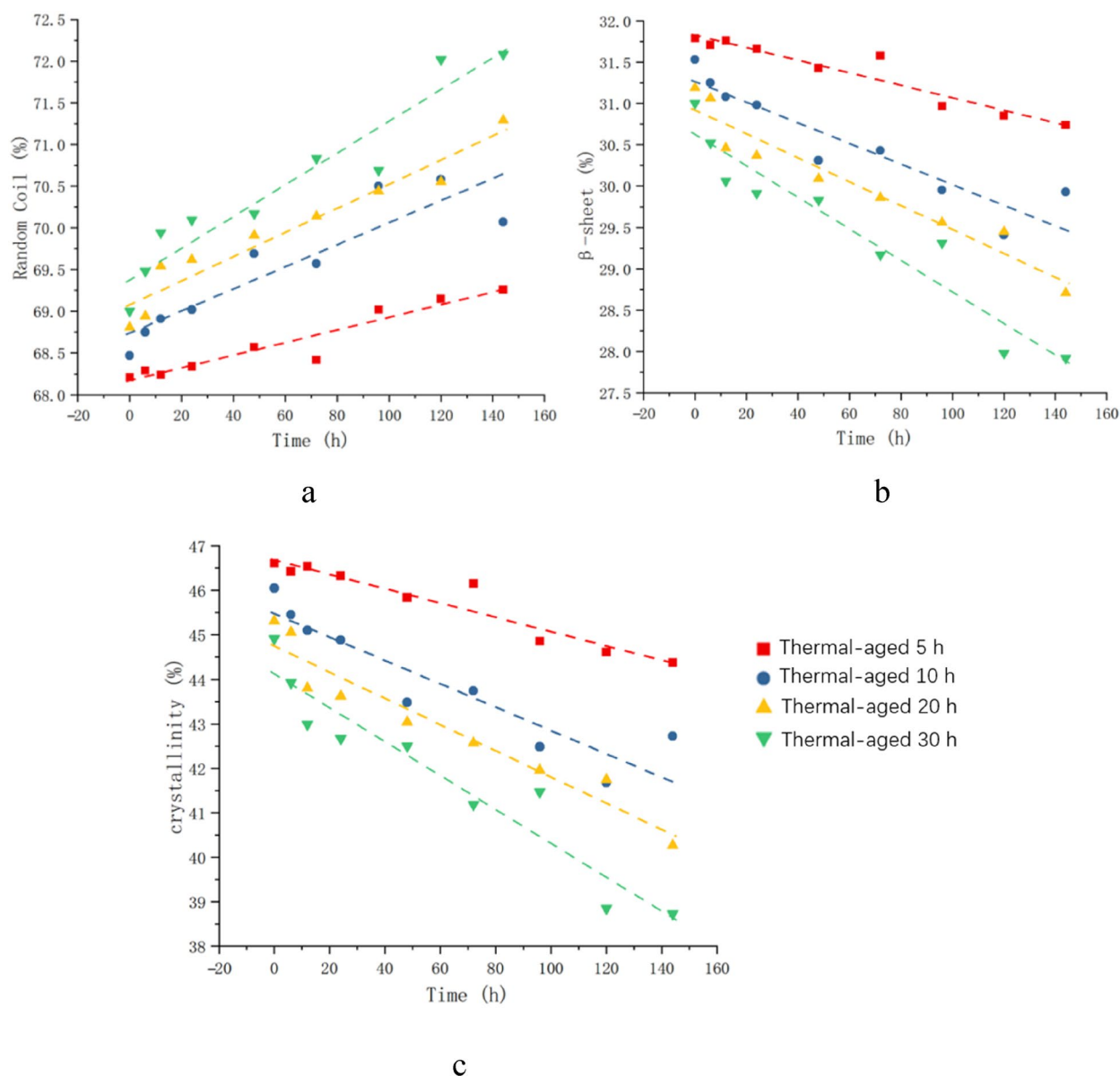
Fig. 4 Variation of the secondary conformation **a**. random coil, **b**. β-sheet) and crystallinity **c** of the aged silk samples

crystallites [34], making the crystalline region more vulnerable to damage. Another possibility is that the selective absorption of light leads to the variation of light energy received by silk with different initial ageing degrees. While the higher initial-aged silk showed a more prominent yellowing appearance indicating it mainly reflects the long wave of the spectrum and absorbs the short wave [22], hence the secondary structure transformation is more pronounced.

^{13}C CPMAS NMR analysis

The ^{13}C CPMAS NMR spectra of each sample group are presented in Fig. 5 along with the chemical shifts and corresponding attributions provided in Table 4. Silk fibroin is predominated by the amino acids of glycine (Gly), alanine (Ala), tyrosine (Tyr) and serine (Ser) [4]. As depicted in Fig. 5 and Table 4, the identified peaks are assigned to carbons of Gly, Ala, Tyr and Ser. Apparently, these peaks appeared at almost identical locations in the unaged and aged silk samples.

Gong *et al. Heritage Science*   (2024) 12:151

Page 10 of 13
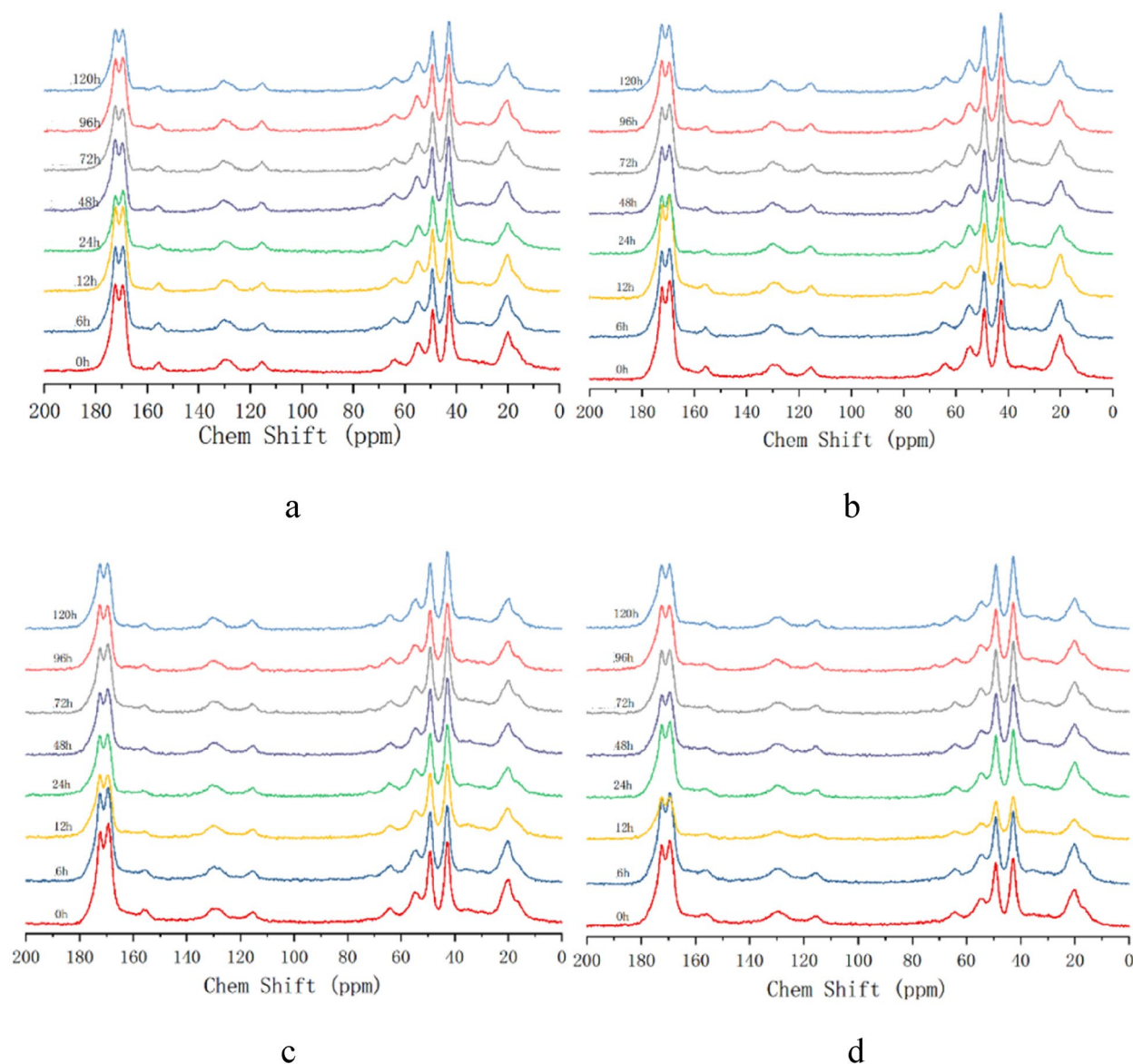
Fig. 5 ^{13}C solid state NMR spectra of each sample group

The individual amino acid has different characteristic carbon atoms leading to distinct resonance absorption peaks in the ^{13}C solid state NMR spectrum. Due to the overlapping of carbonyl resonance regions (Gly C=O, Ala C=O), and Tyr C_α and Ser C_α peaks as a result of the close chemical shift and background noise of some peaks, these peaks were not considered in analysis [35]. After careful comparison, the proportions of absorption peak area near 42 ppm, 49 ppm, 64 ppm and 156 ppm were selected to characterize the relative contents of Gly, Ala, Ser and Tyr, respectively.

The concentrations of amino acids found in each sample group are tabulated in Table 5. As seen from the data, the relative contents of main amino acids varied under experimental lighting. Amongst them, the relative contents of Tyr decreased with the increase of illumination time which is consistent with the previous studies [4, 6]. The degradation of Tyr would produce yellow substance which result in the yellowing effect of silk [36]. As observed in Fig. 6, the variation of relative contents of Tyr was positively correlated with the initial ageing degree of silk, that is, the higher the initial ageing degree, the more rapid the decrease of relative contents of Tyr. Hence, it is

Gong *et al. Heritage Science*   (2024) 12:151

Page 11 of 13

Table 4 ^{13}C chemical shifts and corresponding attributions of each sample group

Samples	Exposure time (h)	Chemical shifts (ppm)									
		Ala C$_\beta$	Gly C$_\alpha$	Ala C$_\alpha$	Ser C$_\alpha$	Ser C$_\beta$	Tyr C$_\epsilon$	Tyr C$_\gamma$	Tyr C$_\xi$	Gly C=O	Ala C=O
Thermal aged 5 h	0	19.99	42.63	49.13	54.88	63.93	115.40	129.30	155.65	169.46	172.50
	6	20.17	42.81	49.24	54.97	64.23	115.51	129.65	155.69	169.29	172.45
	12	20.11	42.81	49.19	54.57	64.12	115.49	129.38	155.45	169.29	172.45
	24	20.00	42.64	49.13	54.84	63.86	115.49	129.72	155.53	169.43	172.48
	48	20.55	43.00	49.30	55.23	64.49	115.81	129.97	155.84	169.54	172.50
	72	20.00	42.78	49.17	54.88	64.01	115.40	129.86	155.86	169.42	172.56
	96	20.46	42.91	49.28	55.17	64.31	115.56	129.50	156.00	169.29	172.45
	120	20.15	42.81	49.21	55.03	64.09	115.51	130.01	155.77	169.37	172.56
Thermal aged 10 h	0	19.84	42.65	69.14	54.66	64.00	115.40	129.25	155.70	169.46	172.50
	6	20.08	42.81	49.21	54.93	64.27	115.61	129.55	155.70	169.29	172.51
	12	19.75	42.62	49.13	54.59	64.18	115.52	129.31	156.18	169.29	172.53
	24	20.30	42.81	49.21	55.00	64.12	115.66	129.64	155.95	169.29	172.51
	48	20.42	42.96	49.35	55.06	64.29	115.72	129.95	155.82	169.48	172.50
	72	20.03	42.88	49.25	55.02	64.18	115.42	129.98	155.72	169.47	172.51
	96	20.43	42.87	49.27	55.11	64.26	115.64	129.68	155.90	169.49	172.54
	120	20.18	42.81	49.13	54.98	64.08	115.73	129.71	155.94	169.34	172.52
Thermal aged 20 h	0	20.11	42.66	49.13	54.72	64.21	115.67	129.31	156.13	169.29	172.54
	6	20.50	42.97	49.33	54.93	64.42	115.67	129.69	155.66	169.29	172.55
	12	20.24	42.81	49.22	54.70	64.33	115.40	129.83	155.66	169.36	172.64
	24	19.75	42.60	49.14	54.69	64.18	115.49	129.59	155.95	169.38	172.52
	48	20.60	43.02	49.42	55.09	64.69	115.76	129.99	156.25	169.29	172.61
	72	19.79	42.64	49.13	54.71	64.06	115.58	129.65	155.37	169.41	172.65
	96	20.22	42.80	49.22	54.88	64.30	115.46	129.60	156.25	169.49	172.52
	120	19.61	42.53	48.97	54.62	63.98	115.61	129.66	155.37	169.49	172.65
Thermal aged 30 h	0	20.00	42.74	49.13	54.41	64.36	155.75	129.58	155.95	169.37	172.67
	6	19.88	42.70	49.13	54.50	64.30	115.82	129.68	156.36	169.37	172.70
	12	20.11	42.81	49.22	54.70	64.42	155.78	129.73	155.37	169.31	172.61
	24	20.32	42.87	49.28	54.93	64.52	116.04	129.87	156.25	169.44	172.60
	48	20.23	42.81	49.24	54.66	64.48	115.84	130.04	155.95	169.29	172.60
	72	19.99	42.76	49.21	54.74	64.26	115.74	129.47	155.07	169.44	172.65
	96	20.41	42.93	49.36	54.87	64.62	115.80	130.05	157.13	169.54	172.65
	120	20.49	42.95	49.37	55.07	64.57	115.64	129.95	156.12	169.50	172.66

inferred that silk with a higher ageing degree was more likely to undergo photooxidation and other reactions, resulting in rapid loss of Tyr. Meanwhile, yellow substance was generated by decomposition of Tyr, leading to the quick yellowing of silk.

Conclusion

In this study, the simulated light ageing experiments were established, and the variation of color and structure of artificially aged silks with different ageing degrees were determined. By comparing the SEM images of each sample group, it is obvious that the higher initial-aged sample is more prone to fracture and other damage traits at an early stage of illumination. After completing 144 h of

light ageing, the higher initial-aged silks were severely delicate with cavities formed inside the fibers.

Upon the extend of exposure time, silk samples with different initial ageing degrees revealed different color variation rate and discoloration tendency. The changes of red concentration and yellow concentration of silk varied greatly, while lower initial-aged silk tended to be less red and yellow, and higher initial-aged silk turned to be red and yellow. Especially at the early stage of illumination, the difference in the sample colorimetric parameter variations was more pronounced due to the rapid photochemical reaction.

The structure of each sample group also exhibited different degradation characteristics under experimental
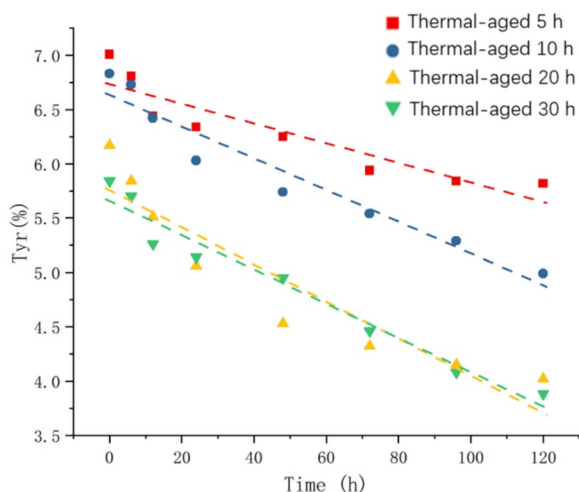
Gong *et al. Heritage Science*   (2024) 12:151

Page 12 of 13

Fig. 6 Relative content variation of Tyr of each sample group

Table 5 Amino acid concentration of each sample group

Samples	Exposure time (h)	Gly (%)	Ala (%)	Ser (%)	Tyr (%)
Thermal aged 5 h	0	44.05	33.59	15.36	7.01
	6	41.70	34.64	16.85	6.81
	12	40.52	38.13	14.90	6.44
	24	42.20	36.36	15.11	6.34
	48	38.24	34.43	21.08	6.25
	72	39.16	35.77	19.13	5.94
	96	38.38	35.80	19.99	5.84
	120	38.55	35.74	19.89	5.82
Thermal aged 10 h	0	39.88	35.05	18.24	6.83
	6	40.70	34.90	17.67	6.73
	12	41.75	34.51	17.32	6.42
	24	38.51	35.67	19.79	6.03
	48	40.31	36.58	17.37	5.74
	72	43.51	34.34	16.51	5.54
	96	40.78	36.02	17.91	5.29
	120	39.56	36.07	19.38	4.99
Thermal aged 20 h	0	42.95	35.52	15.36	6.17
	6	41.29	34.15	18.72	5.84
	12	40.70	36.02	17.76	5.51
	24	42.84	35.72	16.38	5.06
	48	42.24	37.68	15.55	4.53
	72	43.99	38.67	13.02	4.32
	96	43.45	35.42	16.99	4.15
	120	41.51	36.66	17.81	4.02
Thermal aged 30 h	0	41.96	35.27	16.93	5.84
	6	40.89	36.43	16.99	5.70
	12	42.54	34.18	18.01	5.26
	24	43.81	36.38	14.66	5.14
	48	43.80	38.14	13.11	4.95
	72	43.04	40.07	12.43	4.46
	96	42.19	38.81	14.92	4.08
	120	43.38	39.33	13.40	3.88

lighting conditions. By comparing the amid I, amid II and amid III bands in FTIR spectra, the variations of the peak height and position presumably indicating the loss of peptide structure and the transformation from higher-ordered to disordered conformation of the silks upon promoting the light ageing process. The higher initial-aged silk presented higher conversion rate of β-sheet conformation to random coil conformation with more rapid decrease of crystallinity, suggesting the higher disordered structure makes the crystallinity region of silk more vulnerable to light damage. Alternatively, the selective absorption of light causing the variation of light energy received by silk with different pre-ageing degrees. The higher initial-aged silk showed a more prominent yellowing appearance indicating it mainly reflects the long wave of the spectrum and absorbs the short wave, as a result, leads to more pronounced secondary structure transformation. Moreover, the relative contents of main amino acids varied under experimental lighting, while higher initial-aged silk was more likely to undergo photooxidation and other reactions which resulting in the greater loss of Tyr. Since the degradation of Tyr would produce yellow substance, it finally resulted in the quick yellowing of silk.

This work is of significance to understand the long-time impacts of luminous environment on degraded silk and can further serve as a useful reference for predicting the duration of exhibited ancient silk. It is also suggested that in addition to avoid ultraviolet radiation, museums should thoroughly evaluate the ageing degrees of silk cultural relics and estimate reasonable duration of exhibition in order to decelerate the irreversible light damage. Future study could focus on the establishment of light-ageing risk assessment model for the preventive conservation of silk.

Gong *et al. Heritage Science*   (2024) 12:151

Page 13 of 13

Declarations

Ethics approval and consent to participate
Not applicable.

Competing interests
The authors declare no competing interests.

References
1. Li L, Gong DC, Yao ZY, Wang J. A preliminary study of the decline in solubility of ancient silk protein. Polym Degrad Stab. 2019;169: 108988.
2. Wang HY, Zhang YQ, Wei ZG. Characterization of undegraded and degraded silk fibroin and its significant impact on the properties of the resulting silk biomaterials. Intl J Bio Macromolecules. 2021;176:578–88.
3. Gong DC, Yang HY. The discovery of free radicals in ancient silk textiles. Polym Degrad Stab. 2013;98:1780–3.
4. Zhang XM, Berghe IV, Wyeth P. Heat and moisture promoted deterioration of raw silk estimated by amino acid analysis. J Cult Herit. 2011;12:408–11.
5. Tsuboi Y, Ikejiri T, Shiga S, Yamada K, Itaya A. Light can transform the secondary structure of silk protein. Appl Phys A. 2001;73(5):637–40.
6. Gong YX, Li Z, Hu JN, Zhou GZ, Xu GX, Yang WM, Zhang JX. Insight into the measurements for determining the ageing degree of ancient silk. Polym Degrad Stab. 2022;196: 109833. https://doi.org/10.1016/j.polymdegradstab.2022.109833.
7. Koh LD, Cheng Y, Teng CP, Khin YW, Loh XJ, Tee SY, Low M, Ye E, Yu HD, Zhang YW, Han MY. Structures, mechanical properties and applications of silk fibroin materials. Prog Polym Sci. 2015;46:86–110. https://doi.org/10.1016/j.progpolymsci.2015.02.001.
8. Zhou P, Li G, Shao Z, Pan X, Yu T. Structure of Bombyx mori silk fibroin based on the DFT chemical shift calculation. J Phys Chem B. 2001;105(50):12469–76. https://doi.org/10.1021/jp0125395.
9. Gong YX, Li L, Gong DC, Yin H, Zhang JZ. Biomolecular evidence of silk from 8,500 years ago. PLoS ONE. 2016. https://doi.org/10.1371/journal.pone.0168042.
10. Koperska MA, Pawcenis D, Bagniuk J, Zaitz MM, Missori M, Łojewski T, Łojewska J. Degradation markers of fibroin in silk through infrared spectroscopy. Polym Degrad Stab. 2014;105:185–96.
11. Koperska MA, Pawcenis D, Milczarek JM, Blachecki A, Łojewski T, Łojewska J. Fibroin degradation—critical evalution of conventional analytical methods. Polym Degrad Stab. 2015;120:357–67.
12. Zhou XD, Guo YJ, Luo XY, Zhang LF, Wu MQ, Zhang WQ. Systematic assessment of the silk deterioration behaviors for silk aging prediction. Polym Degrad Stab. 2023;218: 110532. https://doi.org/10.1016/j.polymdegradstab.2023.110532.
13. Tan HJ, Dang R. Review of lighting deterioration, lighting quality, and lighting energy saving for paintings in museums. Build Environ. 2022;208: 108608. https://doi.org/10.1016/j.buildenv.2021.108608.
14. Smedemark SH, Ryhl-Svendsen M, Toftum J. Distribution of temperature moisture and organic acids in storage facilities with heritage collections. Build Environ. 2020. https://doi.org/10.1016/j.buildenv.2020.106782.
15. Ferdyn-Grygierek J, Grygierek K. HVAC control methods for drastically improved hygrothermal museum microclimates in warm season. Build Env. 2019;149:90–9. https://doi.org/10.1016/j.buildenv.2018.12.018.
16. Li Z, Zhang JJ, Wang H, Dang R. Indicators for lighting Chinese paintings in museums based on the protection standards and color preferences. Energy & Buildings. 2023;299: 113610. https://doi.org/10.1016/j.enbuild.2023.113610.
17. Dang R, Guo WL, Luo T. Correlated colour temperature index of lighting source for polychrome artworks in museums. Build Environ. 2020;185: 107287. https://doi.org/10.1016/j.buildenv.2020.107287.
18. Ishii M, Moriyama T, Toda M, Kohmoto K, Saito M. Color degradation of textiles with natural dyes and blue scale standards exposed to white LED lamps: evaluation of white LED lamps for effectiveness as museum lighting. J Light & Vis Env. 2008;32(4):370–8.
19. Groeneveld I, Kanelli M, Ariese F, van Bommel MR. Parameters that affect the photodegradation of dyes and pigments in solution and on substrate—an overview. Dyes Pigm. 2023;210: 110999. https://doi.org/10.1016/j.dyepig.2022.110999.
20. Jo S, Ryu SR, Jang W, Kwon OS, Rhee B, Lee YE, Kim D, Kim J, Shin K. LED illumination-induced fading of traditional Korean pigments. J Cult Herit. 2019;37:129–36.
21. Vasileiadou A, Karapanagiotis I, Zotou A. UV-induced degradation of wool and silk dyed with shellfish purple. Dyes Pigm. 2019;168:317–26.
22. Dang R, Zhang FH, Yang D, Guo WL, Liu G. Spectral damage model for lighting paper and silk in museum. J Cult Herit. 2020;45:249–53.
23. Liu HL, Zhao SH, Zhang Q, Yeerken T, Yu WD. Secondary structure transformation and mechanical properties of silk fibers by ultraviolet irradiation and water. Textile Res J. 2018;89(14):2802.
24. Li MY, Zhao Y, Tong T, Hou XH, Fang BS, Wu SQ, Shen XY, Tong H. Study of the degradation mechanism of Chinese historic silk (*Bombyx mori*) for the purpose of conservation. Polym Degrad Stab. 2013;98:727–35.
25. Cai YL, Jia LJ, Li H, He YJ, Liu Y, Jia R, Yang D, Xia RT, Jiao JP, Huang J, Weng Y, Zhang JC, Zheng HL, Yang HL, Wang B, Zhou Y, Peng ZQ. Structure and stable isotope ratios of ancient and artificially aged silk fabrics. Polym Degrad Stab. 2023;218: 110576. https://doi.org/10.1016/j.polymdegradstab.2023.110576.
26. Commission Internationale de l'Éclairage (CIE) CIE 157:2004—control of damage to museum objects by optical radiation. CIE. Vienna.
27. Mangkuto RA, Simamora TP, Pratiwi DP, Koerniawan MD. Computational modelling and simulation to mitigate the risk of daylight exposure in tropical museum buildings. Energy and Build Env. 2024;5:171–84.
28. National standard of China GB/T 23863:2009—Code for lighting design of museum, China, 2009
29. Luxford N, Thickett D. Designing accelerated ageing experiments to study silk deterioration in historic houses. J Inst Conserv. 2011;34(1):115–27.
30. Kim J, Wyeth P. Towards a routine methodology for assessing the condition of historic silk. E-Preserv Sci. 2009;6:60–7.
31. Zhang XN, Gong DC, Gong YX. Insight into the orientation behavior of thermal-aged and historic silk fabrics by polarized FTIR microspectroscopy. J Cult Herit. 2019;38:53–63.
32. Koperska MA, Łojewski T, Łojewska J. Evaluating degradation of silk's fibroin by attenuated total reflectance infrared spectroscopy: case study of ancient banners from polish collections. Spectrochim Acta Part A Mol Biomol Spectrosc. 2015;135:576–82.
33. Shao JD, Zheng JH, Liu JQ, Carr CM. Fourier transform raman and fourier transform infrared spectroscopy studies of silk fibroin. J Appl Polym Sci. 2005;96(6):1999–2004.
34. Garside P, Wyeth P. Crystallinity and degradation of silk: correlations between analytical signatures and physical condition on ageing. Appl Physics A. 2007;89:871–6.
35. Wishart DS, Bigam CG, Holm A, Hodges RS, Sykes BD. [1]H, ^{13}C and ^{15}N random coil NMR chemical shifts of the common amino acids. I. Investigations of nearest-neighbor effects, J. biomolecular NMR 5 (1995) 67–81.
36. Vassileva V, Baltova S, Handjieva S. Photochemical behaviour of natural silk—III photofading of silk dyed with acid azo dyes. Polym Degrad Stab. 1998;61(3):367–73.

Publisher's Note